The synthesis and complex anion-vacancy ordered structure of $La_{0.33}Sr_{0.67}MnO_{2.42}$

Edward Dixon [a], Joke Hadermann [b], Michael A. Hayward [a,*]

[a] *Department of Chemistry, Inorganic Chemistry Laboratory, University of Oxford, South Parks Road, Oxford OX1 3QR, United Kingdom*
[b] *EMAT, University of Antwerp, Groenenborgerlaan 171, B-2020 Antwerp, Belgium*

ABSTRACT

The low-temperature topotactic reduction of $La_{0.33}Sr_{0.67}MnO_3$ with NaH results in the formation of $La_{0.33}Sr_{0.67}MnO_{2.42}$. A combination of neutron powder and electron diffraction data show that $La_{0.33}Sr_{0.67}MnO_{2.42}$ adopts a novel anion-vacancy ordered structure with a 6-layer OOTOOT' stacking sequence of the 'octahedral' and tetrahedral layers ($Pcmb$, $a=5.5804(1)$ Å, $b=23.4104(7)$ Å, $c=11.2441(3)$ Å). A significant concentration of anion vacancies at the anion site, which links neighbouring 'octahedral' layers means that only 25% of the 'octahedral' manganese coordination sites actually have 6-fold MnO_6 coordination, the remainder being MnO_5 square-based pyramidal sites. The chains of cooperatively twisted apex-linked MnO_4 tetrahedra adopt an ordered -L–R–L–R- arrangement within each tetrahedral layer. This is the first published example of a fully refined structure of this type which exhibits such intralayer ordering of the twisted tetrahedral chains. The rationale behind the contrasting structures of $La_{0.33}Sr_{0.67}MnO_{2.42}$ and other previously reported reduced $La_{1-x}Sr_xMnO_{3-y}$ phases is discussed.

© 2011 Elsevier Inc. All rights reserved.

1. Introduction

Complex manganese oxides have been the subject of intense study, since the observation of large mangetoresistive ratios in materials with mixed valent $Mn^{3+/4+}$ centres [1–3]. Interest has been sustained in the electronic and magnetic behaviour of these materials by the observation of strong coupling between spin, charge and lattice degrees of freedom [4,5]. In addition wider attention has focused on mixed valent manganates, particularly anion-deficient phases of the form $La_{1-x}Sr_xMnO_{3-y}$, due to their potential application as mixed ionic/electronic conductors in solid oxide fuel cell (SOFC) cathodes and other devices [6].

This combination of strongly correlated electronic behaviour and mixed ionic/electronic conductivity has motivated a number of studies focusing on the structural chemistry (anion-vacancy ordering) and electronic behaviour of anion-deficient manganese oxides based on the cubic perovskite structure. Limiting ourselves to a discussion of anion-deficient phases based on strontium doped $LaMnO_3$, it is useful to divide these $La_{1-x}Sr_xMnO_{3-y}$ materials into two groups: those with $x \leq 0.5$ and those with $x > 0.5$. Considering the lanthanum rich group first, topotactic reduction of $La_{1-x}Sr_xMnO_3$ phases with x in the range $0.2 \leq x \leq 0.5$ results in the

formation of anion-deficient materials of composition $La_{1-x}Sr_xMnO_{2.5}$ which adopt brownmillerite-type, anion-vacancy ordered structures with average manganese oxidation states in the range $Mn^+2.2$–$Mn^+2.5$ [7–9]. As shown in Fig. 1 the brownmillerite structure accommodates anion vacancies within the simple ABO_3 cubic perovskite framework by removing half the oxide anions from alternate BO_2 layers to yield a structure with an -AO–BO_2–AO–BO- stacking sequence of alternating layers of apex-linked BO_6 octahedra and BO_4 tetrahedra. The anion vacancies within the BO layers are aligned in chains parallel to the [1 1 0] direction of the simple cubic perovskite sublattice. As a result the BO_4 tetrahedra within these layers also form apex-linked chains which run parallel to the [1 1 0] direction. These chains of tetrahedra can undergo a cooperative twist in one of two possible senses to yield either a 'left' or 'right' handed chain—the two being related by symmetry. The three dimensional patterning of the tetrahedral chain twist direction leads to a large number of distinct structural configurations [10], the most common five of which are shown in Fig. 1 [8].

In contrast to the lanthanum rich $La_{1-x}Sr_xMnO_{3-y}$ phases, anion-deficient phases reported for strontium rich substrates ($x > 0.5$) are significantly less reduced, having average manganese oxidation states in the range $Mn^+2.84$–Mn^+4 and structures constructed from MnO_5 square-based pyramids and MnO_6 octahedra as shown in Fig. 2 [11–13]. In order to determine if the observed higher oxidation states and lower anion deficiency of strontium rich $La_{1-x}Sr_xMnO_{3-y}$ phases indicates a stability boundary, or only that
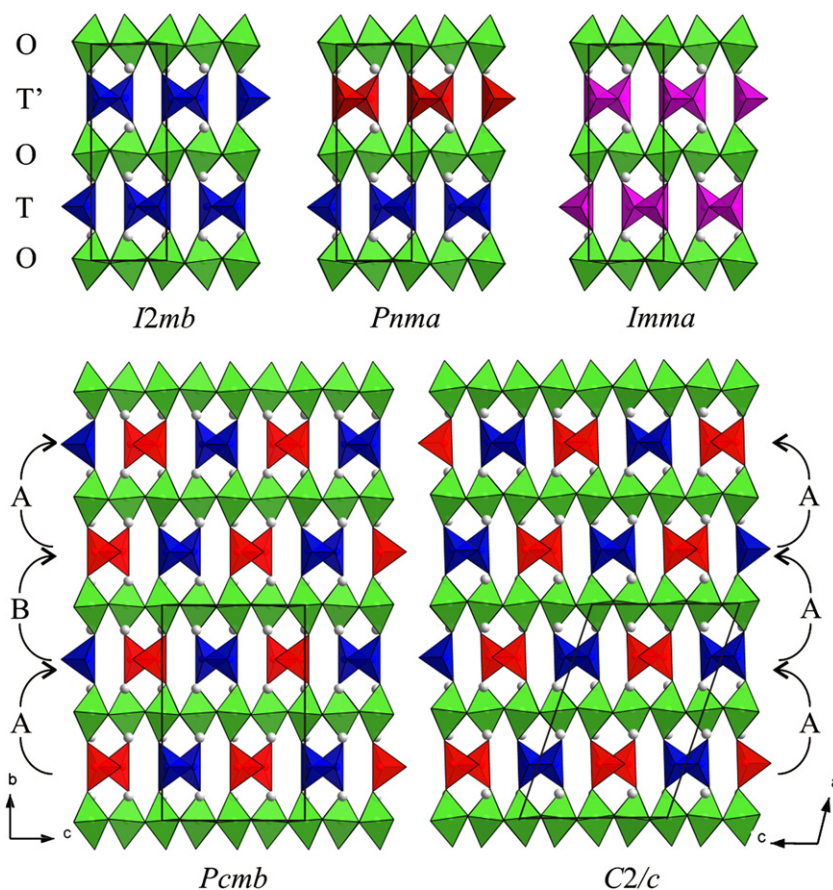
Fig. 1. Five common variants of the brownmillerite structure. Colours indicate the relative 'twist' direction of the tetrahedral chains. (For interpretation of the references to color in this figure legend, the reader is referred to the web version of this article.)
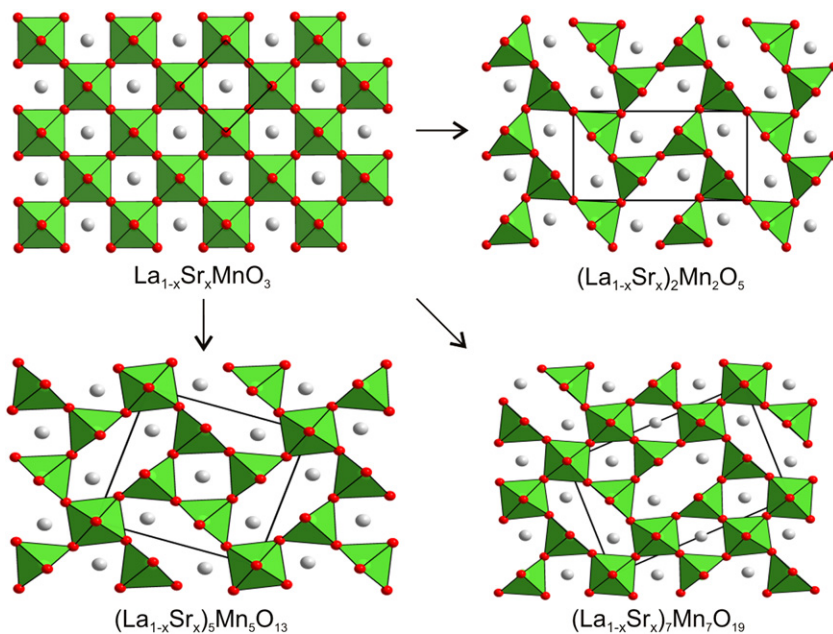
Fig. 2. Structures of the three anion vacancy ordered structures reported for $La_{1-x}Sr_xMnO_{3-y}$ ($x > 0.5$) phases [7–9].

a more powerful chemical agent is required to reduce these phases, we undertook a study of the topotactic reduction chemistry of $La_{1-x}Sr_xMnO_3$ ($x > 0.5$) substrates with the powerful solid-state reducing agent NaH [14]. Here we report the synthesis and structural characterisation of $La_{0.33}Sr_{0.67}MnO_{2.42}$ which exhibits a novel 6-layer variant of the brownmillerite structure.

2. Experimental

2.1. Preparation of $La_{0.33}Sr_{0.67}MnO_3$

Samples of $La_{0.33}Sr_{0.67}MnO_3$ were prepared using a standard ceramic route as previously described by Chmaissem et al. [15]. Appropriate stoichiometric ratios of La_2O_3 (99.999%, dried at 900 °C), $SrCO_3$ (99.994%) and MnO_2 (99.999%) were thoroughly mixed and then heated at 900 °C under flowing argon to decompose the carbonate. The resulting black powder was reground, pressed into 13 mm pellets with a force of 5 tonnes and then heated at 1350 °C for 3 periods of 48 h under flowing argon with intermittent grinding. Finally, the powder was heated to 400 °C under flowing oxygen for 12 h and cooled to room temperature at 1 °C min^{-1} to ensure full oxygen stoichiometry was achieved. X-ray powder diffraction data collected from this material were consistent with a single phase with lattice parameters ($a=3.8394(1)$ Å) consistent with those previously reported for the $La_{1-x}Sr_xMnO_3$ series [15].

2.2. Reduction of $La_{0.33}Sr_{0.67}MnO_3$

The reduction of $La_{0.33}Sr_{0.67}MnO_3$ was performed using NaH (> 95%) as a solid-state reducing agent [14]. Approximately 4 g of $La_{0.33}Sr_{0.67}MnO_3$ was mixed with two mole equivalents of NaH in an argon-filled glove box (O_2 and $H_2O < 1$ ppm). The resulting mixture was then sealed under vacuum in a Pyrex tube and heated for 24 h at 180 °C and then for a further 24 h at 210 °C. The sample was reground and then heated at 210 °C for a further 3 periods of 48 h with intermittent regrinding. Finally the sample was washed under a nitrogen atmosphere with 4×100 ml of methanol to remove sodium containing phases (NaOH and NaH) before being dried under vacuum.

2.3. Characterisation methods

X-ray powder diffraction data were collected using a PANalytical X'Pert diffractometer incorporating an X'celerator position sensitive detector (monochromatic Cu $K\alpha1$ radiation). Neutron powder diffraction data were collected using the D2b diffractometer (ILL neutron source, Grenoble) at a wavelength of $\lambda=1.59$ Å from a sample contained within a vanadium can sealed under an argon atmosphere with an indium washer. Rietveld profile refinement was performed using the GSAS suite of programs [16]. Electron diffraction data were collected from finely ground samples supported on holey carbon grids (deposited from suspension in ethanol) using a Philips CM20 microscope. Thermogravimetric reoxidation measurements were performed by heating powdered samples under flowing oxygen using a Netzsch STA 409PC balance.

3. Results

3.1. Structural and chemical characterisation

X-ray powder diffraction data collected from $La_{0.33}Sr_{0.67}MnO_{3-y}$ (Fig. 3a) could be readily indexed on the basis of an orthorhombic unit cell, related to that of a simple cubic perovskite structure by means of a $\sqrt{2}a_p \times 3a_p \times \sqrt{2}a_p$ expansion, suggesting a topotactic reduction had occurred. Close inspection of these X-ray powder diffraction data revealed rather broad and poorly resolved diffraction peaks, especially at high angle, attributable to slight disorder within the anion sublattice of the phase. Therefore, in order to improve the crystallinity of samples, various annealing experiments were performed. These experiments
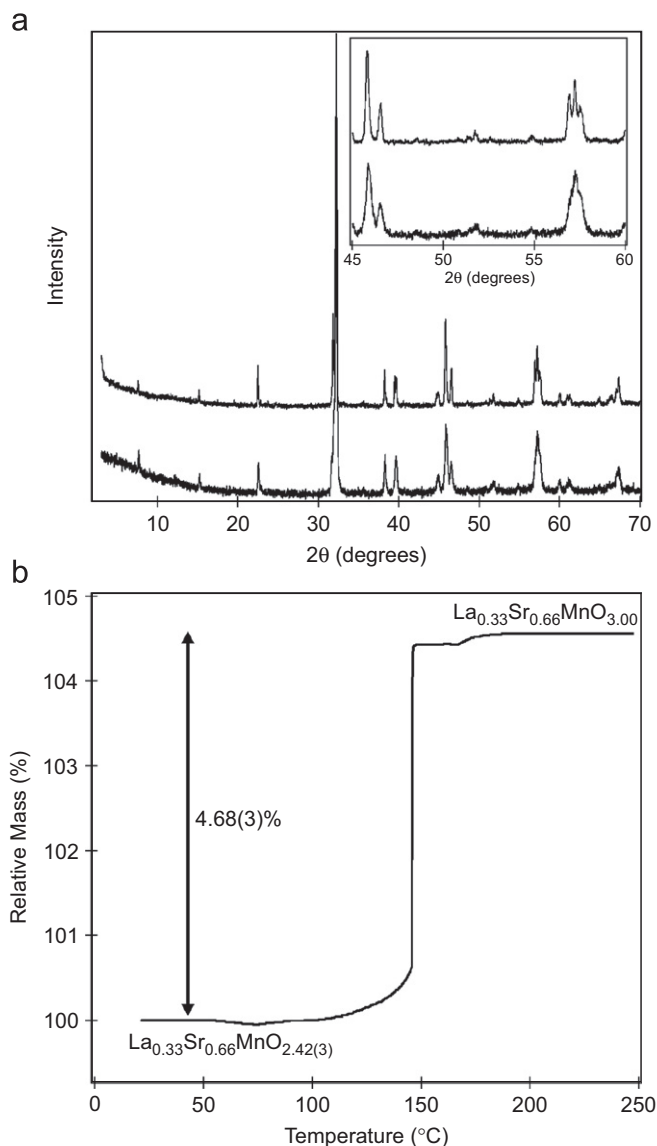
Fig. 3. (a) X-ray powder diffraction data collected from annealed (top) and unannealed (bottom) samples of $La_{0.33}Sr_{0.67}MnO_{2.42}$ and (b) thermogravimetric data collected during the oxidation of an annealed sample of $La_{0.33}Sr_{0.67}MnO_{2.42(3)}$ to $La_{0.33}Sr_{0.67}MnO_3$.

indicated that heating samples at 400 °C in sealed, evacuated silica ampoules was the optimum regime: below this temperature, there was no improvement in the crystallinity of the sample and above this temperature, mild decomposition to the substituent binary oxides occurred. X-ray powder diffraction data collected from a sample annealed under this regime are also shown in Fig. 3a for comparison.

Thermogravimetric data collected during the reoxidation of an annealed sample of $La_{0.33}Sr_{0.67}MnO_{3-y}$ to $La_{0.33}Sr_{0.67}MnO_{3.00}$ (confirmed by X-ray powder diffraction) are consistent with an empirical stoichiometry of $La_{0.33}Sr_{0.67}MnO_{2.42(3)}$ (Fig. 3b) and an average manganese oxidation state of Mn+2.5.

The $\sqrt{2}a_p \times 3a_p \times \sqrt{2}a_p$ lattice expansion deduced from X-ray powder diffraction data for $La_{0.33}Sr_{0.67}MnO_{2.42}$ is consistent with an anion-vacancy ordered structure based on that of $(La_{1/3}Ca_{2/3})_3Fe_3O_8$ [17] or, with a further doubling of the b lattice parameter, that of $RESr_2GaCu_2O_7$ (RE=Y, lanthanide)[18] as shown in Fig. 4. The poor sensitivity of X-ray powder diffraction data to the location of light anions (oxide) in the presence of heavy cations

(lanthanum and strontium) prevent an unambiguous determination of the unit cell of $La_{0.33}Sr_{0.67}MnO_{2.42}$. Therefore, in order to confirm the true size and symmetry of the crystallographic unit cell of $La_{0.33}Sr_{0.67}MnO_{2.42}$, electron diffraction data were collected.

The structures of both $(La_{1/3}Ca_{2/3})_3Fe_3O_8$ and $RESr_2GaCu_2O_7$ can be considered as 3 or 6-layer analogues of the $A_2B_2O_5$ brownmillerite structure as shown by comparing Figs. 1 and 4. In previous structural studies of brownmillerite phases, D'Hondt

Fig. 4. Anion vacancy ordered structures of 3-layer $(La_{1/3}Ca_{2/3})_3Fe_3O_8$ and 6-layer $RESrGaCu_2O_7$ (RE=Y, lanthanide) [17,8]

et al. demonstrated that electron diffraction data collected from brownmillerite phases could be usefully indexed using a set of four indices, $hklm$, in which the diffraction vector is $\mathbf{g}=h\mathbf{a}^*+k\mathbf{b}^*+l\mathbf{c}^*+m\mathbf{q}$ with either $\mathbf{q}=\beta\mathbf{b}^*+\gamma\mathbf{c}^*$ in the (3+1)D space group $I2/m(0\ \beta\ \gamma)0s$ or $\mathbf{q}=\gamma\mathbf{c}^*$ in the (3+1)D space group $Imma(0\ 0\ \gamma)s00$ [10]. Due to the structural similarities between 3-layer $(La_{1/3}Ca_{2/3})_3Fe_3O_8$, 6-layer $RESr_2GaCu_2O_7$ and the 4-layer brownmillerite structure, a similar procedure was used to index the electron diffraction data collected from $La_{0.33}Sr_{0.67}MnO_{2.42}$.

Close inspection of the electron diffraction data collected from $La_{0.33}Sr_{0.67}MnO_{2.42}$ (Fig. 5) revealed a number of diffraction features, which are inconsistent with the unit cell derived from X-ray powder diffraction data. Careful analysis of these features using the incommensurate classification described above yielded a unit cell consistent with a (3+1)D model with $Imma(0\ 0\ \gamma)s00$ superspace group symmetry with $\gamma=\frac{1}{2}$. This indexation is consistent with a 3D model with a $\sqrt{2}a_p \times 6a_p \times 2\sqrt{2}a_p$ unit cell expansion relative to the unit cell of the simple cubic perovskite structure and, according to Table 2 in Ref. [10], $Pcmb$, $Pcma$ or $Pcm2_1$ symmetry.

The 6-fold expansion of the unit cell parallel to the y-axis suggests that $La_{0.33}Sr_{0.67}MnO_{2.42}$ adopts a 6-layer anion-vacancy ordered structure based on that of $RESr_2GaCu_2O_7$ [18]. Furthermore the observed cell expansion of $La_{0.33}Sr_{0.67}MnO_{2.42}$ in the xz-plane ($\sqrt{2}a_p \times 6a_p \times 2\sqrt{2}a_p$) is directly analogous to the $\sqrt{2}a_p \times 4a_p \times 2\sqrt{2}a_p$ unit cell expansions observed for the 4-layer brownmillerite phases $La_{0.65}Sr_{0.35}MnO_{2.5}$ and $La_{0.6}Sr_{0.4}MnO_{2.5}$ [8]. These brownmillerite phases crystallise in space group $Pcmb$ and exhibit ordered alternating arrangements of 'left' and 'right' twisted tetrahedral chains within the tetrahedral layers of their structures as shown in Fig. 1. Thus the observed unit cell expansion suggests that $La_{0.33}Sr_{0.67}MnO_{2.42}$ exhibits an anion-vacancy

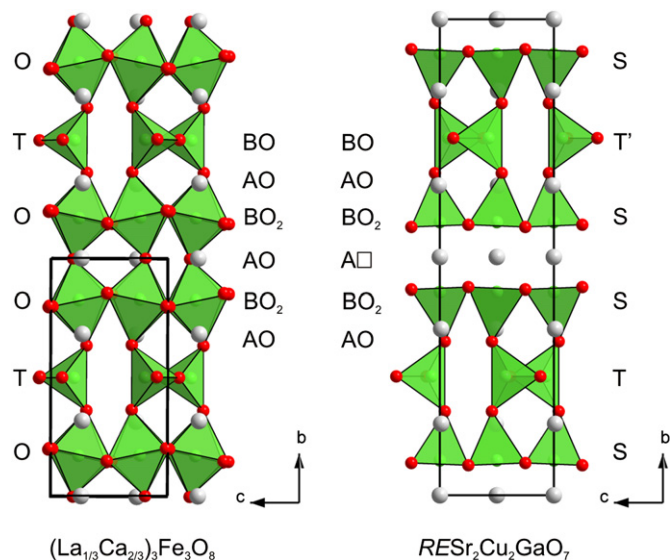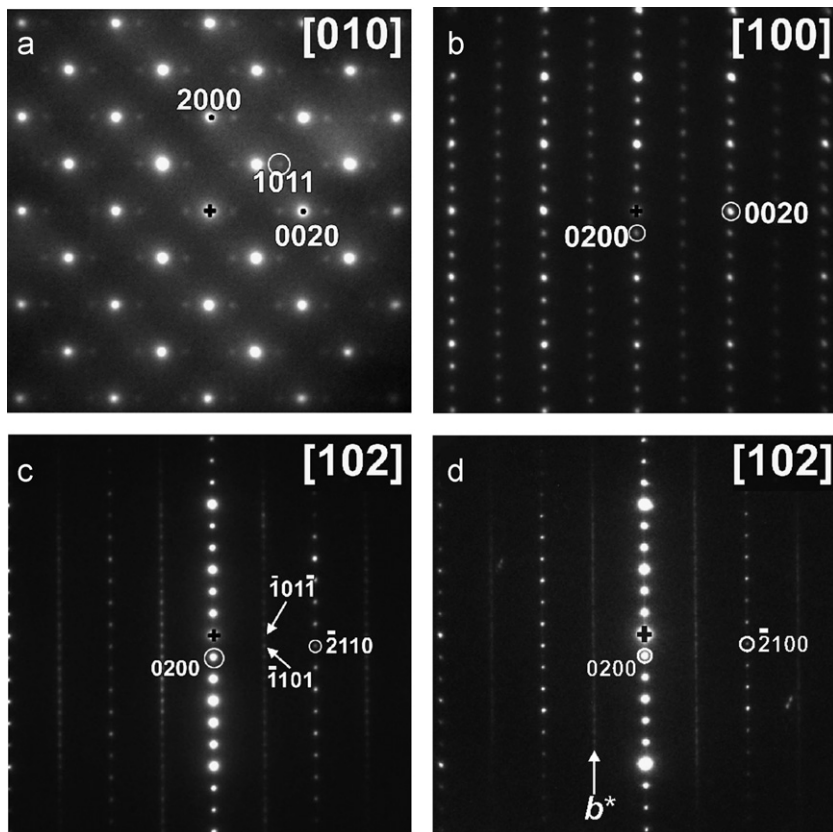**Fig. 5.** Electron diffraction data collected from the (a) [0 1 0], (b) [1 0 0] and (c) [1 0 2] zone axes of $La_{0.33}Sr_{0.67}MnO_{2.42}$. (d) shows data collected from the [1 0 2] zone axis of $La_{0.33}Sr_{0.67}MnO_{2.42}$ exhibiting streaking parallel to the b^* direction.

ordered structure based on that of $RESr_2GaCu_2O_7$ but with an alternating -L–R–L–R- arrangement of tetrahedral chains analogous to $La_{0.65}Sr_{0.35}MnO_{2.5}$ and $La_{0.6}Sr_{0.4}MnO_{2.5}$.

Building on this information a series of structural models were constructed by starting with the structure of $RESr_2GaCu_2O_7$ (Fig. 4) and adding an additional oxide ion site located between the square-pyramidal layers to generate two octahedral layers and an overall stoichiometry of $A_3B_3O_8$. Then the five different tetrahedral chain ordering patterns commonly observed in brownmillerite phases (Fig. 1) [8] were incorporated to generate five distinct structural models (Fig. 6). Specifically models were constructed in space groups $I2mb$, $Pnma$ and $Imma$ (with unit cells expanded by $\sqrt{2}a_p \times 6a_p \times \sqrt{2}a_p$ relative to a simple cubic perovskite), $Pcmb$ (with a $\sqrt{2}a_p \times 6a_p \times 2\sqrt{2}a_p$ cell expansion) and $C2/c$ (with a monoclinic unit cell) [8]. These models were refined against the neutron powder diffraction data collected from $La_{0.33}Sr_{0.67}MnO_{2.42}$ to establish if the expanded unit cell determined from the electron diffraction data described the long range structure of $La_{0.33}Sr_{0.67}MnO_{2.42}$ or just short range ordering.

During the refinement of these models all atomic positional and thermal parameters were allowed to vary. In addition, to account for the oxygen non-stoichiometry of the reduced phase (i.e. the chemically determined stoichiometry $(La_{0.33}Sr_{0.67})_3$ $Mn_3O_{7.26}$ rather than $A_3B_3O_8$) the fractional occupancies of all the anion sites were also allowed to vary. While the majority of anion sites remained fully occupied within error, the occupancy of the 'bridging' anion site(s) (labelled O(1) and O(8) in Fig. 8) rapidly declined in all 5 models, with an improvement in the fit

to the data in each case. The occupancies of these bridging anion sites declined to values which indicated a slightly greater anion deficiency than the stoichiometry determined by thermogravimetric data. Therefore in order to be consistent with the composition determined chemically the occupancies of these sites were set and fixed to give an overall stoichiometry of $La_{0.33}Sr_{0.67}Mn$ $O_{2.42}$ for the refined structural models.

It can be seen from the fitting statistics in Table 1 that the best fit to the neutron diffraction data was achieved using the model in space group $Pcmb$, consistent with the electron diffraction data. However, close inspection of a small number of electron diffraction patterns collected from $La_{0.33}Sr_{0.67}MnO_{2.42}$ revealed slight streaking along the $b*$ direction (Fig. 5). This observation is consistent with mild disorder parallel to this crystallographic direction,

Table 1

Fitting statistics for the refinement of 6-layer models against neutron powder diffraction data collected from $La_{0.33}Sr_{0.67}MnO_{2.42}$.

Space group	χ^2	wR_p (%)	R_p (%)	Structural parameters	Global parameters
$I2mb$	3.519	5.31	4.17	26	30
$Imma$	2.967	4.88	3.87	26	30
$Pnma$	3.394	5.22	4.12	26	30
$C2/c$	2.916	4.83	3.81	45	30
$Pcmb$	2.862	4.81	3.80	44	30
Disordered $Pcmb$	2.715	4.65	3.68	45	30
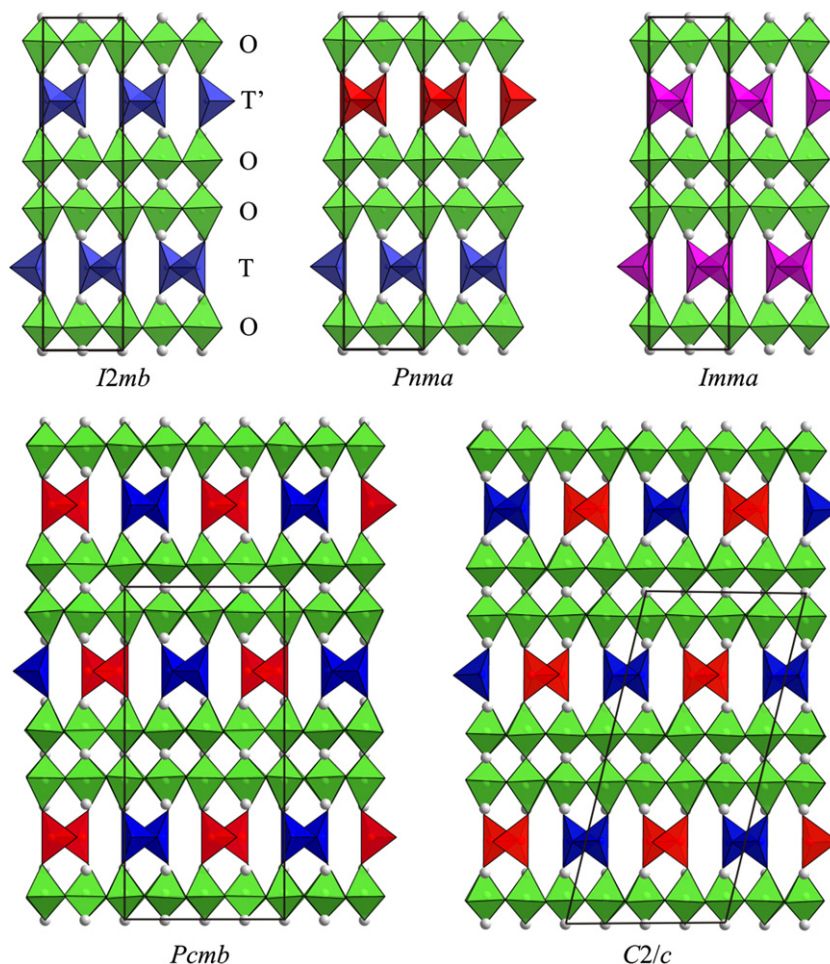
Fig. 6. Five different 6-layer $A_3Mn_3O_8$ structural models refined against neutron diffraction data. The models incorporate the five common tetrahedral twist orderings observed in brownmillerite phases (see Fig. 1).

suggestive of a disordered stacking along the b-axis of rigorously ordered ac layers (no streaking along a^* or c^* directions).

There are two obvious sources of this stacking disorder. Firstly it could arise from a deviation of the rigorous 'staggering' of the tetrahedral chains between adjacent layers. This would mean that rather than the ordered OOTOOT' 6-layer stacking sequence of the $RESr_2GaCu_2O_7$ structure [18], there could be intergrowths of 3-layer OOTOOT stacking as observed in the structure of $(La_{1/3}Ca_{2/3})_3Fe_3O_8$ (Fig. 4) [17] Alternatively the observed disorder could arise from 'faults' in the ordered array of twisted tetrahedral chains brought about by deviations from the rigorous ABAB stacking of the tetrahedral sheets, defined by the $Pcmb$ space-group, by the inclusion of some AA stacking typical of the $C2/c$ brownmillerite structure type (Fig. 1).

To determine if either of these stacking defects were present in the structure of $La_{0.33}Sr_{0.67}MnO_{2.42}$, models were constructed based on modifications to the ordered $Pcmb$ model (i) with additional oxide ions present within the tetrahedral layers of the model to represent the positions of oxide ions in 'eclipsed' tetrahedral chains (such disorder has been observed in the structure of $(La_{1/3}Sr_{2/3})_3Fe_3O_8$) [19] or (ii) with additional oxide ions present within the tetrahedral layers of the model to represent the positions of oxide ions in tetrahedral chains with the opposite twist to those of the ordered $Pcmb$ model, similar to the $Imma$ brownmillerite structural variant. In both disordered models constraints were applied to make all tetrahedral chains symmetrically equivalent.

These two disordered structural models were refined against the neutron powder diffraction data by allowing the fractional occupancies of all the oxide ions within the tetrahedral layers to vary. The refinement of the disordered model describing the staggered/eclipsed disordering process was found to be highly unstable, with the occupancies of the defect sites rapidly declining to zero, so this model was discarded. The second defect model, however, describing faults in the tetrahedral chain twist direction, rapidly converged to give a good fit to the data. This model was refined against the neutron powder diffraction data and yielded a statistically better fit to the data than the 'ordered' $Pcmb$ model ($\chi^2 = 2.715$ vs $\chi^2 = 2.862$, Table 1). A complete description of the refined structure of $La_{0.33}Sr_{0.67}MnO_{2.42}$ is given in Table 2, with selected bond lengths and bond valence sums in Table 3. Observed calculated and difference plots from the refinement are shown in Fig. 7. The complex magnetic behaviour of $La_{0.33}Sr_{0.67}MnO_{2.42}$ will be described elsewhere.

4. Discussion

Previous studies of the topotactic reduction of phases in the composition range $La_{1-x}Sr_xMnO_3$ ($0.5 < x \leq 1$) using hydrogen as a reducing agent yielded materials with modest levels of reduction [11–13]. For example the reduction of $La_{0.4}Sr_{0.6}MnO_3$ and $La_{0.3}Sr_{0.7}MnO_3$ with hydrogen yields $La_{0.4}Sr_{0.6}MnO_{2.62(1)}$ ($Mn+2.84$) and $La_{0.3}Sr_{0.7}MnO_{2.62(1)}$ ($Mn+2.92$), respectively [12]. The oxygen stoichiometries of these two phases indicate an average manganese coordination number of ~ 5.2, which in the case of $La_{0.3}Sr_{0.7}MnO_{2.62}$ is accounted for by an ordered array of 6-coordinate octahedral and 5-coordinate pyramidal manganese coordination sites as shown in Fig. 2.

The topotactic reduction of $La_{0.33}Sr_{0.67}MnO_3$ with NaH described in this study, leads to much greater levels of reduction, yielding a phase of composition $La_{0.33}Sr_{0.67}MnO_{2.42}$ with an average manganese oxidation state of $Mn+2.5$. The greater degree of oxygen deintercalation induced into $La_{0.33}Sr_{0.67}MnO_{2.42}$

Table 3
Selected bond lengths and angle from the structural refinement of $La_{0.33}Sr_{0.67}MnO_{2.42}$. Bond valence sums: Mn (2) and Mn(2′)=1.909; Mn(3) and Mn(3′)=2.034.

| Atom	Bond	Length (Å)	Bond	Length (Å)
Mn octahedral	Mn(1)–O(1)	1.897(23)	Mn(4)–O(5)	1.997(27)
	Mn(1)–O(2)	2.057(33)	Mn(4)–O(6)	1.940(24)
	Mn(1)–O(5)	1.997(31)	Mn(4)–O(7)	2.073(33)
	Mn(1)–O(6)	2.049(29)	Mn(4)–O(8)	1.896(23)
	Mn(1)–O(9)	2.031(31)	Mn(4)–O(9)	1.984(27)
	Mn(1)–O(10)	2.015(31)	Mn(4)–O(10)	1.977(27)
Mn tetrahedral	Mn(2)–O(3)	2.183(36)	Mn(3)–O(3)	2.063(19)
	Mn(2)–O(4)	2.262(32)	Mn(3)–O(4)	1.926(32)
	Mn(2)–O(7) × 2	1.954(24)	Mn(3)–O(2) × 2	2.101(23)
Tetrahedral twist	O(3)–O(4)–O(3)	112.69(80)		

Table 2
Structural parameters refined against neutron powder diffraction data collected from $La_{0.33}Sr_{0.67}MnO_{2.42}$.

Atom	Wyckoff position	x	y	z	Occupancy	U_{iso} (Å³)
La/Sr(1)	4a	½	0	0	0.33/0.67	0.002(1)
La/Sr(2)	4c	0.996(3)	0	¼	0.33/0.67	0.002(1)
La/Sr(3)	8e	0.499(2)	0.155(1)	0.992(1)	0.33/0.67	0.002(1)
La/Sr(4)	8e	0.998(2)	0.151(1)	0.254(1)	0.33/0.67	0.002(1)
Mn(1)	8e	0.002(5)	0.081(1)	0.997(2)	1	0.001(1)
Mn(2)	4d	0.535(5)	³/₄	0.265(2)	0.76(2)	0.001(1)
Mn(2')	4d	0.464(5)	³/₄	0.265(2)	0.24(2)	0.001(1)
Mn(3)	4d	0.057(4)	¼	0.039(1)	0.76(2)	0.001(1)
Mn(3')	4d	0.942(4)	¼	0.039(1)	0.24(2)	0.001(1)
Mn(4)	8e	0.504(3)	0.081(1)	0.250(2)	1	0.001(1)
O(1)	4a	0	0	0	0.25	0.41(5)
O(2)	8e	0.969(2)	0.168(1)	0.977(1)	1	0.006(1)
O(3)	4d	0.923(4)	¼	0.210(1)	0.76(2)	0.006(1)
O(3')	4d	0.076(4)	¼	0.210(1)	0.24(2)	0.006(1)
O(4)	4d	0.402(4)	¼	0.045(2)	0.76(2)	0.006(1)
O(4')	4d	0.597(4)	¼	0.045(2)	0.24(2)	0.006(1)
O(5)	8e	0.750(4)	0.064(1)	0.374(1)	1	0.006(1)
O(6)	8e	0.244(3)	0.072(1)	0.363(1)	1	0.006(1)
O(7)	8e	0.476(2)	0.169(1)	0.265(1)	1	0.006(1)
O(8)	4c	½	0	¼	0.25	0.41(5)
O(9)	8e	0.254(4)	0.072(1)	0.126(1)	1	0.006(1)
O(10)	8e	0.745(4)	0.074(1)	0.122(1)	1	0.006(1)

$La_{0.33}Sr_{0.67}MnO_{2.42}$: space group $Pcmb$, $a=5.5804(1)$ Å, $b=23.4104(7)$ Å, $c=11.2441(3)$ Å, cell volume$=1648.9(1)$ Å³ MnO: space group $Fm\bar{3}m$, $a=4.447(1)$ Å; wt. frac.$=1.5(1)$ % $\chi^2=2.715$, $wR_p=4.65\%$, $R_p=3.68\%$.
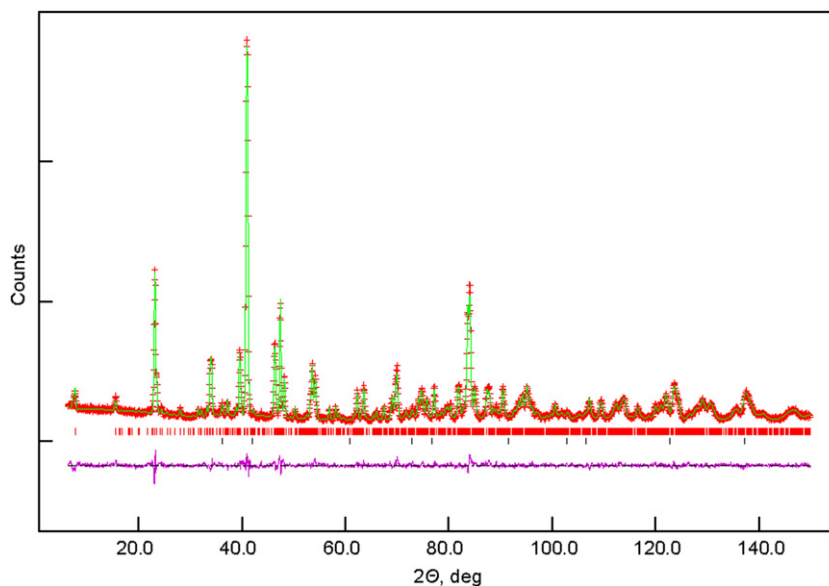
Fig. 7. Observed, calculated and difference plots from the structural refinement of $La_{0.33}Sr_{0.67}MnO_{2.42}$. Upper tick marks indicate peak positions from the majority phase, lower tick marks from a small quantity (1.5wt%) of MnO present in the sample.

using NaH as a reducing agent, results in the average manganese coordination number dropping to 4.84. This means that there must now be some 4-coordinate manganese centres within the structure of the reduced material produced. Neutron and electron diffraction data indicate $La_{0.33}Sr_{0.67}MnO_{2.42}$ adopts a novel anion-vacancy ordered structure constructed from tetrahedral and octahedral/pyramidal layers stacked in an ordered OOTOOT' sequence as shown in Fig. 8. The low occupancy of the anion sites which bridge between the 'octahedral' layers (O(1) and O(8)) means that only 25% of the cations in the 'O' octahedral layers actually have 6-fold coordination, with the remaining 75% occupying 5-coordinate pyramidal sites. In addition the large displacement parameters refined for the O(1) and O(8) bridging anions (Table 2) indicate appreciable disorder within the bridging anion layer, consistent with significant local relaxation of the anion positions within this layer to maximise bonding interactions.

The structure adopted by $La_{0.33}Sr_{0.67}MnO_{2.42}$ can be considered as a 6-layer analogue of the 4-layer brownmillerite type structures shown in Fig. 1. Using this analogy it can be seen that the chains of tetrahedra in the OOTOOT' structure of $La_{0.33}Sr_{0.67}$ $MnO_{2.42}$ can undergo the same cooperative twisting as the equivalent chains in the OTOT' brownmillerite structures and as a result can exhibit the same complex tetrahedral chain twist ordering schemes observed in the latter structure type. Neutron and electron diffraction data indicate that $La_{0.33}Sr_{0.67}MnO_{2.42}$ adopts a structure in which the tetrahedral chain twist direction alternates within each tetrahedral layer (Fig. 8) in a manner directly analogous to that of the $Pcmb$ variant of the brownmillerite structure (Fig. 1). Previous work has shown that the different tetrahedral chain twist ordering schemes adopted by the different brownmillerite structural variants can be accounted for on the basis of the cancellation of dipole moments which arise from the twisting of the tetrahedral chains themselves [20,21], with the specific structural variant adopted being a function of chain dipole size (degree of tetrahedral chain twisting), tetrahedral layer separation, and in the specific case of $La_{1−x}Sr_xMnO_{2.5}$ phases, the degree of octahedral $Mn^{2+/3+}$ charge order [8]. The degree of tetrahedral chain distortion as indicated by the O–O–O angle of the equatorial oxide ions which run along each tetrahedral chain [8], (O(3)–O(4)–O(3) in the case of $La_{0.33}Sr_{0.67}$ $MnO_{2.42}$) has a value of 112.7° for $La_{0.33}Sr_{67}MnO_{2.42}$ (Table 3).
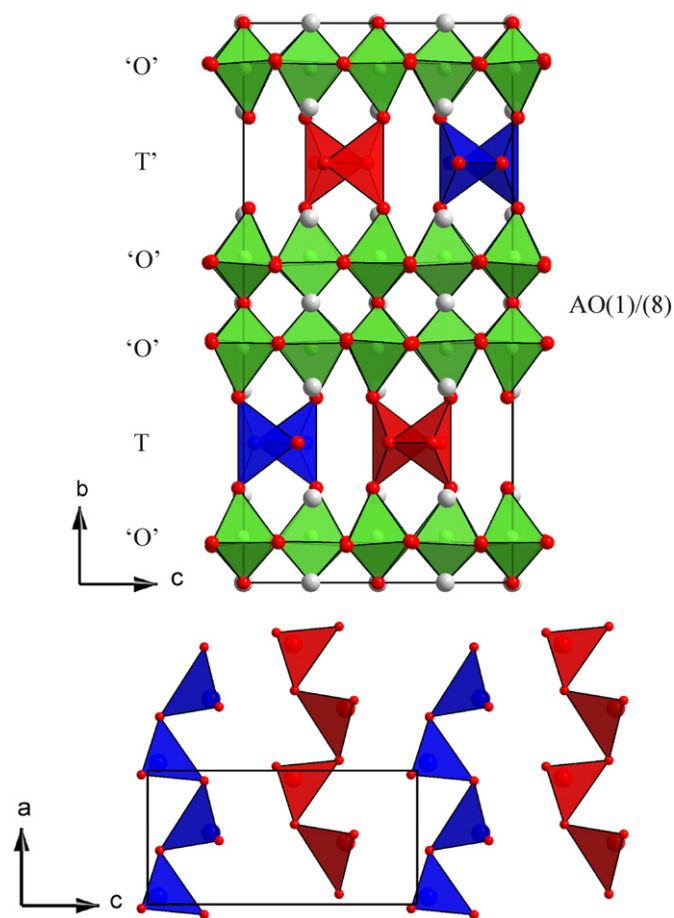
Fig. 8. (Top) The refined structure of $La_{0.33}Sr_{0.67}MnO_{2.42}$. Anion sites O(1) and O(8) are 25% occupied. (bottom) A view down the b-axis of an -L–R–L–R- ordered T layer. The slight disorder present in these sheets is omitted for clarity.

This value falls within the range of distortion angles observed for intralayer ordered $La_{1−x}Sr_xMnO_{2.5}$ brownmillerite phases (111.8°—116.2° for $Pcmb$ and $C2/c$ variants) [8] suggesting a dipole cancellation mechanism similar to that proposed for the

brownmillerite phases is responsible for the tetrahedral chain order in $La_{0.33}Sr_{0.67}MnO_{2.42}$. It should be noted that $La_{0.33}Sr_{0.67}MnO_{2.42}$ is not the first 6-layer phase for which a structure containing ordered -L–R–L–R- tetrahedral sheets has been proposed. An analogous intralayer ordered structural arrangement has been suggested for $YSr_2CoCu_2O_7$ on the basis of electron diffraction data [22], however, to the best of our knowledge $La_{0.33}Sr_{0.67}MnO_{2.42}$ is the first 6-layer phase for which such an ordered structure has been refined.

The tetrahedral chain twist ordering scheme refined for $La_{0.33}Sr_{0.67}MnO_{2.42}$ contains a significant degree of disorder arising from faults in the rigorous ABAB stacking of the ordered layers of tetrahedra. This disorder clearly indicates that the interactions which structurally couple adjacent tetrahedral layers, and drive the ordered stacking, are weakened in $La_{0.33}Sr_{0.67}MnO_{2.42}$. This is not surprising given the large spatial separation between the tetrahedral layers and the presence of a disordered anion-deficient layer between adjacent sheets of tetrahedra. We therefore believe that the observed disorder in the stacking of the tetrahedral layers is intrinsic to $La_{0.33}Sr_{0.67}MnO_{2.42}$ and separate from the crystallographic disorder which was 'removed' by post-reaction annealing of the sample.

Given the near ubiquity of phases adopting brownmillerite structures and the observation that the reduction of phases in the compositional range $La_{1-x}Sr_xMnO_3$ $(0.2 \leq x \leq 0.5)$ results in reduced materials which adopt 4-layer brownmillerite type structures [7,8], it is pertinent to ask: why does the reduction of $La_{0.33}Sr_{0.67}MnO_3$ not result in the formation of the hypothetical brownmillerite type phase $La_{0.33}Sr_{0.67}MnO_{2.5}$? Some light can be shed on this issue by considering the structures of the $La_{1-x}Sr_xMnO_{2.5}$ $(0.2 \leq x \leq 0.5)$ brownmillerite type phases in detail. Bond valence sum calculations [23] indicate that the tetrahedral manganese coordination sites within these $La_{1-x}Sr_xMnO_{2.5}$ $(0.2 \leq x \leq 0.5)$ brownmillerite phases are occupied exclusively by Mn^{2+} centres, with the remaining octahedral sites occupied by a mixture of Mn^{2+} and Mn^{3+} centres in a proportion defined by the La:Sr ratio [7,8]. The hypothetical phase $La_{0.33}Sr_{0.67}MnO_{2.5}$ would have an average manganese oxidation state of $Mn+2.67$ and as a consequence, if this phase were to adopt a brownmillerite type structure, it would require some Mn^{3+} cations to be located within tetrahedral sites. This situation is highly unfavourable on CFSE and electrostatic grounds as demonstrated by the adoption of the 'normal' spinel structure by Mn_3O_4 and the disproportionation of Mn^{3+} to Mn^{2+} and Mn^{4+} within the spinel $NiMn_2O_4$ [24,25]. This leads us to suggest

that in contrast to the lanthanum rich end of the $La_{1-x}Sr_xMnO_3$ solid solution, reduction of $La_{0.33}Sr_{0.67}MnO_3$ does not lead to the formation of a brownmillerite type phase so as to avoid the formation of a tetrahedral Mn^{3+} site. Instead a 6-layer structure is adopted in which the inclusion of an additional 'octahedral' layer into the stacking sequence removes the need to locate Mn^{3+} centres on tetrahedral sites, as shown in Fig. 9. Based on this argument we also expect that brownmillerite phases will not be formed as products of the reduction of $La_{1-x}Sr_xMnO_3$ phases where $x > 0.5$.

5. Conclusion

The formation of $La_{0.33}Sr_{0.67}MnO_{2.42}$ via the reduction of $La_{0.33}Sr_{0.67}MnO_3$, clearly demonstrates that highly reduced phases can be prepared by the reduction of $La_{1-x}Sr_xMnO_3$ $(x > 0.5)$ substrates if sufficiently powerful reducing agents are used. The 6-layer anion-vacancy ordered structure adopted by $La_{0.33}Sr_{0.67}MnO_{2.42}$ has a flexible anion content (via the partial occupation of the anion sites which link neighbouring 'octahedral' layers) suggesting it will be formed over a wide range of La:Sr ratios. Furthermore the adoption of this 6-layer structure in preference to the more common 4-layer brownmillerite structure – a preference we propose is driven by the coordination preferences of different manganese oxidation states – reaffirms the importance of electronic/lattice coupling in directing and determining the structure and anion mobility of anion deficient manganese perovskites.

Acknowledgement

References

[1] K. Chahara, T. Ohno, M. Kasao, Y. Kozono, Appl. Phys. Lett. 63 (1993) 1990.
[2] R. von Helmolt, J. Wecker, B. Holzapfel, L. Schultz, K. Sanwer, Phys. Rev. Lett. 71 (1993) 2331.
[3] P. Schiffer, A.P. Ramirez, W. Bao, S.-W. Cheong, Phys. Rev. Lett. 75 (1995) 3336.
[4] C.N.R. Rao, A.K. Cheetham, R. Mahesh, Chem. Mater. 8 (1996) 2421.
[5] B. Raveau, A. Maignan, C. Martin, M. Hervieu, Chem. Mater. 10 (1998) 2641.
[6] S.P. Jiang, J. Mater. Sci. 43 (2008) 6799.
[7] P.S. Casey, D. Barker, M.A. Hayward, J. Solid State Chem. 179 (2006) 1375–1382.
[8] T.G. Parsons, H. D'Hondt, J. Hadermann, M.A. Hayward, Chem. Mater. 21 (2009) 5527.
[9] R. Cortes-Gil, M.L. Ruiz-Gonzalez, J.M. Alonso, M. Vallet-Regi, M. Hernando, J.M.Gonzalez Calbet, Chem. Eur. J. 13 (2007) 4246–4252.
[10] H. D'Hondt, A.M. Abakumov, J. Hadermann, A.S. Kalyuzhnaya, M.G. Rozova, E.V. Antipov, G. Van Tendeloo, Chem. Mater. 20 (2008) 7188–7194.
[11] L. Suescun, B. Dabrowski, J. Mais, S. Remsen, J.W. Richardson, E.R. Maxey, J.D. Jorgensen, Chem. Mater. 20 (2008) 1636–1645.
[12] L. Suescun, D. Dabrowski, S. Remsen, J. Mais, J. Solid State Chem. 182 (2009) 187–195.
[13] T. Mori, N. Kamegashira, J. Alloys Compds. 408-412 ((2006) 1210.
[14] M.A. Hayward, M.A. Green, M.J. Rosseinsky, J. Sloan, J. Am. Chem. Soc. 121 (1999) 8843–8854.
[15] O. Chmaissem, D. Dabrowski, S. Kolesnik, J. Mais, J.D. Jorgensen, S. Short, Phys. Rev. B 67 (2003) 94431.
[16] A.C. Larson, R.B. Von Dreele, Los Alamos National Laboratory Report LAUR 86-748, 2000.
[17] J.M. Hudspeth, D.J. Goossens, A.J. Studer, R.L. Withers, L. Noren, J. Phys.:Condens. Matter 21 (2009).
[18] G. Roth, P. Adelmann, G. Heger, R. Knitter, T. Wolf, J. Phys. I 1 (1991) 721–741.
[19] P.D. Battle, T.C. Gibb, P. Lightfoot, J. Solid State Chem. 84 (1990) 237.
[20] A.M. Abakumov, A.S. Kalyuzhnaya, M.G. Rozova, E.V. Antipov, J. Hadermann, G. Van Tendeloo, Solid State Sci. 7 (2005) 801–811.
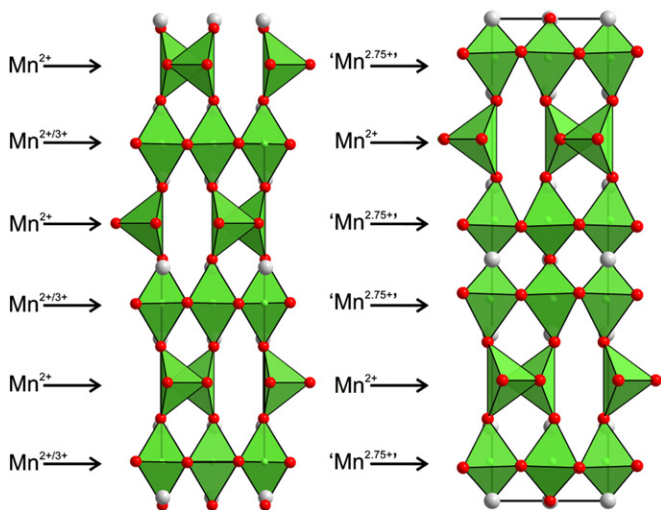
Fig. 9. Manganese charge ordering schemes in $La_{1-x}Sr_xMnO_{2.5}$ $(0.2 \leq x \leq 0.5)$ (left) and $La_{0.33}Sr_{0.67}MnO_{2.42}$ (right).

[21] J. Hadermann, A.M. Abakumov, H. D'Hondt, A.S. Kalyuzhnaya, M.G. Rozova, M.M. Markina, M.G. Mikheev, N. Tristan, R. Klingeler, B. Buchner, E.V. Antipov, J. Mater. Chem. 17 (2007) 692–698.

[22] T. Krekels, O. Milat, G. Van Tendeloo, S. Amelinckx, T.G.N. Babu, A.J. Wright, C. Greaves, J. Solid State Chem. 105 (1993) 313–335.

[23] N.E. Brese, M. O'Keeffee, Acta Crystallogr., Sect. B : Struct. Sci. B 47 (1991) 192–197.

[24] G. Aminoff, Zeitschrift fuer Kristallographie, Kristallgeometrie, Kristallphysik, Kristallchemie 64 (1926) 475–490.

[25] A.P.B. Sinha, N.R. Sanjana, A.B. Biswas, Acta Crystallogr 10 (1957) 439–440.